Numerical methods for $p-harmonic$ flows and applications to image processing

Luminita A. Vese* and Stanley J. Osher †

UCLA CAM Report 01-22, August 2001

Department of Mathematics
University of California, Los Angeles
405 Hilgard Avenue
Los Angeles, CA 90095-1555, USA
E-mail: lvese@math.ucla.edu, sjo@math.ucla.edu

Abstract

We propose in this paper an alternative approach for computing $p-$harmonic maps and flows: instead of solving a constrained minimization problem on S^{N-1}, we solve an unconstrained minimization problem, on the entire space of functions. This is possible, using the projection on the sphere, of any arbitrary function. Then, we show how this formulation can be used in practice, for problems with both isotropic and anisotropic diffusion, with applications to image processing, using a new finite difference scheme.

Keywords: energy minimization, $p-harmonic$ maps, $p-harmonic$ flows, directional diffusion, heat flow, total variation minimization, partial differential equations, finite differences, denoising.

1 Introduction

This paper is concerned with the minimization of constrained functionals, and in particular with $p-$harmonic maps. This problem has applications to liquid crystals, as well as to directional diffusion and chromaticity denoising.

Let $\Omega \subset I\!R^M$ be an open and bounded domain, and let S^{N-1} be the unit sphere in $I\!R^N$, for $M \geq 1$ and $N \geq 2$.

We first recall the following notations and terminology. The Euclidean norm of a vector y will be denoted by $|\cdot|$. The vector-valued function $U : \Omega \to I\!R^N$ belongs to S^{N-1}, if and only if, $|U(x)| = 1$, a.e. (for almost every) $x \in \Omega$.

*Supported by NSF ITR-0113439, NSF DMS-9973341 and ONR N00014-02-1-0015.
†Supported by NSF DMS-0074735 and ONR N00014-97-1-0027.

The component gradient ∇U_i and its Euclidean norm are, respectively, defined by:

$$\nabla U_i = \Big(\frac{\partial U_i}{\partial x_1}, \frac{\partial U_i}{\partial x_2}, ..., \frac{\partial U_i}{\partial x_M}\Big),\ |\nabla U_i| = \sqrt{\Big(\frac{\partial U_i}{\partial x_1}\Big)^2 + \Big(\frac{\partial U_i}{\partial x_2}\Big)^2 + ... + \Big(\frac{\partial U_i}{\partial x_M}\Big)^2},$$

and the gradient matrix and its norm of the vector-valued function U are respectively defined by:

$$\nabla U = \begin{pmatrix} \nabla U_1 \\ : \\ \nabla U_N \end{pmatrix} = \begin{pmatrix} \frac{\partial U_1}{\partial x_1} & ... & \frac{\partial U_1}{\partial x_M} \\ : & & : \\ \frac{\partial U_N}{\partial x_1} & ... & \frac{\partial U_N}{\partial x_M} \end{pmatrix},\ |\nabla U| = \sqrt{\sum_{i=1}^{N}\sum_{j=1}^{M}\Big(\frac{\partial U_i}{\partial x_j}\Big)^2}.$$

For $U : \Omega \to S^{N-1}$ and $p \geq 1$, we consider the $p-$energy

$$E_p(U) = \int_\Omega |\nabla U|^p dx, \tag{1}$$

which is finite if U belongs to the Sobolev class $W^{1,p}(\Omega, S^{N-1}) = \{U \in W^{1,p}(\Omega, I\!R^N),\ |U| = 1 \text{ a.e.}\}$.

Minimizing E_p over $U : \Omega \to S^{N-1}$, with associated boundary conditions on $\partial\Omega$, is a constrained minimization problem. Mappings which are stationary for E_p are called $p-harmonic$ maps.

The associated boundary conditions can be, for example: $U|_{\partial\Omega}$ equals a given map in $S^{N-1}(\partial\Omega)$, or the Neumann boundary conditions $\frac{\partial U}{\partial \vec{n}}|_{\partial\Omega} = 0$, where $\vec{n}$ denotes the exterior unit normal to $\partial\Omega$.

Many authors have studied harmonic maps between manifolds (existence, uniqueness or non-uniqueness, regularity; essentially most of them worked on the case $p = 2$): F. Bethuel, H. Brezis and J.M. Coron [5]; F. Bethuel, H. Brezis and F. Helein [6], [7]; R. Schoen and K. Uhlenbeck [27], [28], [29]; M. Struwe [31], [32], [33]; P. Courilleau and F. Demengel [14]; J.-M. Coron and R. Gulliver [13]; H. Brezis, J.-M. Coron and E.H. Lieb [8], and others. There are fewer results for the case $p = 1$ (for example by Giaquinta et al. [18]).

This paper deals with alternative formulations and numerical methods for computing harmonic maps.

There are difficulties of finding numerically the minimizers or the $p-harmonic$ maps, due to non-convexity (the constraint $|U(x)| = 1$ a.e. is not convex), non-regularity and non-uniqueness of minimizers.

There are several classical approaches used to solve the minimization problem (1).

A first approach is to solve the Euler-Lagrange equations associated with the minimization problem. These consist of a set of coupled PDE's:

$$-\text{div}(|\nabla U|^{p-2}\nabla U) = U|\nabla U|^p. \tag{2}$$

The above system of equations holds, if and only if, $U \in S^{N-1}$. However in practice, the numerical solution does not necessarily satisfy the constraint $|U| = 1$ everywhere. To correct the numerical error, several authors ([17], [35], [36]) replace the solution U_*^n obtained at each iteration n, by $U^n = \frac{U_*^n}{|U_*^n|}$, but then the question is whether one still decreases the energy. In this framework, we also refer the reader to [12]. It is known [1] that the energy decrease is guaranteed after this re-normalization if $|U_*^n| \geq 1$, but the behavior of the energy is not

known if $|U_*^n| < 1$. Also, if we would like to extend this numerical procedure involving the projection at each step to other manifolds, then the energy decrease is guaranteed only when the manifold is the boundary of a convex set, and again, if in addition, U_*^n does not belong to the interior of that convex domain.

This problem has been solved in [1] for the S^2 case and in three dimensions, where an interesting convergent algorithm is proposed, but it still involves a re-normalization step at each iteration (ensuring now that the energy decreases after the re-normalization step). Numerical methods for $p-harmonic$ flows are also proposed in [17] and [12], again based on the re-normalization procedure at each step.

The second classical approach is given by the Ginzburg-Landau functionals [6], [7]. Here, the problem is solved by approximation, to eliminate the constraint. The minimization of the energy E_p from (1) under the constraint $|U(x)| = 1$ a.e., is approximated by the unconstrained minimization of the following energies, as $\varepsilon \to 0$:

$$E_\varepsilon(U) = \int_\Omega |\nabla U|^p dx + \frac{1}{\varepsilon}\int_\Omega (1-|U|^2)^2 dx. \tag{3}$$

In this paper, we introduce a different approach to solving minimization problems on S^{N-1}. We solve an unconstrained minimization problem, on the entire space of functions, and not only on S^{N-1}. The method uses the projection of an arbitrary function V to the sphere S^{N-1}. We will present our alternative approach for the case of S^{N-1}. Then, we discuss how this approach can be extended to more general manifolds, and in particular to manifolds defined implicitly, via a level set function. By proposing numerical schemes in the S^1 and S^2 cases, we also show how our formulations can be used in practice, and in particular for applications to directional diffusion and color image denoising.

In the framework of image processing and directional diffusion, related works are [23], [30], [9], [35], [20], [36], [39], and [25], [26]. We also refer to [16] for manifold constrained variational problems. In the framework of energy minimization with values in S^2, we refer the reader to [15], where the algorithm from [1] is applied, in the presence of a data term.

Our main idea is as follows. For $U : \Omega \to S^{N-1}$, with $\Omega \subset I\!R^M$, consider $V : \Omega \to I\!R^N \setminus \vec{0}$, such that

$$U = \frac{V}{|V|}.$$

We minimize without constraint the corresponding energy with respect to V:

$$\inf_V \Big\{F(V) = \int_\Omega \Big|\nabla\Big(\frac{V}{|V|}\Big)\Big|^p dx\Big\}, \tag{4}$$

and then recover U, a minimizer of (1), projecting back on S^{N-1}, by: $U = \frac{V}{|V|}$, where V is a minimizer of (4).

We would like to mention that the idea of solving constrained minimization problems for harmonic maps by associating unconstrained minimization problems, has been used as a theoretical tool by Chen-Lin [10] and Struwe [34]. They find a smooth energy-minimizing harmonic map U as weak limit of minimizers U_L to an unconstrained variational problem, for $L \to \infty$.

The outline of the paper is as follows. In section 2 we consider the S^1 case: we derive the Euler-Lagrange equations associated with the unconstrained minimization problem, and

in subsection 2.1 we propose a numerical scheme for this case. Similarly, section 3 and subsection 3.1 are devoted to the S^2 case. In Section 4 we validate the proposed models and numerical schemes on several experimental results: in 4.1 we consider the case with prescribed boundary conditions, and we make a comparison with the classical formulation (2) with re-normalization step at each iteration (we will see that, by the proposed approach, the numerical accuracy is improved in a test case where we know the exact solution); in section 4.2, we consider the case of directional diffusion, with Neumann boundary conditions, and applications to chromaticity denoising for color images. Finally, we end the paper with a short concluding section and a discussion for more general manifolds.

2 The S^1 case

To develop our main idea, let us first consider the particular case $N = 2$ of S^1. Then, for $U : \Omega \to S^1$, consider $V = (u, v) : \Omega \to I\!R^2$, such that $U = \frac{V}{|V|}$.

In order to obtain in an elegant way the Euler-Lagrange equations associated with the minimization problem (4), we consider the orientation formulation (but which is not always equivalent with the directional formulation). Let $U = (\cos\theta, \sin\theta)$, and $V = (r\cos\theta, r\sin\theta)$. Then $u^2 + v^2 = r^2$ and we have

$$\Big|\nabla\Big(\frac{V}{|V|}\Big)\Big|^2 = |\nabla\theta|^2.$$

For $p = 2$ (the heat flow for harmonic maps), solving

$$\inf_\theta \int_\Omega |\nabla\theta|^2 dx,$$

and parameterizing the descent direction by an artificial time t, we obtain (denoting $u_t = \frac{\partial u}{\partial t}$, $v_t = \frac{\partial v}{\partial t}$):

$$\theta_t = \triangle\theta,\ r_t = 0.$$

Using

$$\theta = \tan^{-1}\Big(\frac{v}{u}\Big),\quad \nabla\theta = \frac{u\nabla v - v\nabla u}{u^2 + v^2},$$

we first deduce that:

$$\frac{uv_t - vu_t}{u^2 + v^2} = \mathrm{div}\Big(\frac{u\nabla v - v\nabla u}{u^2 + v^2}\Big).$$

Now, using $uu_t + vv_t = 0$ (from $r_t = 0$), we obtain the associated Euler-Lagrange equations for $p = 2$:

$$u_t = -v\mathrm{div}\Big(\frac{u\nabla v - v\nabla u}{u^2 + v^2}\Big),\quad v_t = +u\mathrm{div}\Big(\frac{u\nabla v - v\nabla u}{u^2 + v^2}\Big). \tag{5}$$

For $p = 1$ (the total variation minimization of Rudin-Osher-Fatemi [24]), on solving

$$\inf_\theta \int_\Omega |\nabla\theta| dx,$$

we obtain:

$$\theta_t = \mathrm{div}\Big(\frac{\nabla\theta}{|\nabla\theta|}\Big),\ r_t = 0.$$

Then, in a similar way, the associated Euler-Lagrange equations for $p = 1$ are:

$$u_t = -v\mathrm{div}\Big(\frac{u\nabla v - v\nabla u}{|u\nabla v - v\nabla u|}\Big), \quad v_t = +u\mathrm{div}\Big(\frac{u\nabla v - v\nabla u}{|u\nabla v - v\nabla u|}\Big). \tag{6}$$

In the general case, i.e. for any $p \geq 1$, the corresponding linear system in u_t and v_t is:

$$\begin{aligned} uu_t + vv_t &= 0, \\ \frac{uv_t - vu_t}{u^2+v^2} &= \mathrm{div}\Big[\Big(\frac{|u\nabla v - v\nabla u|}{u^2+v^2}\Big)^{p-2}\Big(\frac{u\nabla v - v\nabla u}{u^2+v^2}\Big)\Big]. \end{aligned}$$

Solving this linear system in the unknowns u_t and v_t, yields similar equations in u and v, like those for the cases $p = 2$ and $p = 1$ from (5) and (6) respectively.

We will associate with the problems (5) and (6) initial conditions in the form: $u(0, x) = u_0(x)$ and $v(0, x) = v_0(x)$ in Ω; at the boundary, we can prescribe either Dirichlet boundary conditions $V(t, x)/|V(t, x)| = F(x)$, with $F : \partial\Omega \to S^1$ given, for $t \geq 0$ and $x \in \partial\Omega$; or Neumann boundary conditions $\frac{\partial u}{\partial \vec{n}} = 0$ and $\frac{\partial v}{\partial \vec{n}} = 0$ on $\partial\Omega$.

We could add data terms in the energy, as in [9] or [15].

Remark: With these formulations, with both $p = 1$ and $p = 2$ (and in fact for any $p \geq 1$), we always have, for any fixed $x \in \Omega$: $u(t, x)u_t(t, x)+v(t, x)v_t(t, x) = 0$, or $u^2(t, x)+v^2(t, x) =$ constant in time, for fixed x.

Remark: Note that we have used an artificial time, even if we compute a stationary solution of the problem. This is a common technique, and this artificial time represents a parametrization of the descent direction. It can be shown in general that the energy is decreasing in time, under such a time-dependent flow, for both Dirichlet or Neumann boundary conditions (as explained in detail in the Appendix).

2.1 The numerical algorithm for the S^1 case

To discretize the systems (5) and (6), we use finite differences. Assume for simplicity that $U : [0, 1]^M \to S^1$, let h be the space step, and $\triangle t$ the time step. We denote by u^n and v^n the approximations of $u(n\triangle t, x)$ and of $v(n\triangle t, x)$ respectively, where x is a grid point (to simplify the notation, we will not explicitly indicate the discrete point $x_{i,j}$ where the approximation is considered; for instance, if $M = 2$, u^n means $u^n_{i,j}$, etc; similarly, any expression of the form $(E)^n$ denotes an approximation of the quantity E at $(n\triangle t, x)$, at the same discrete point x; this notational convention will allow us to consider any dimension $M \geq 1$).

We use the following semi-implicit scheme for (5) ($p = 2$):

$$\begin{aligned} \frac{u^{n+1} - u^n}{\triangle t} &= -\frac{v^{n+1} + v^n}{2}\Big[\mathrm{div}\Big(\frac{u\nabla v - v\nabla u}{u^2+v^2}\Big)\Big]^n, \\ \frac{v^{n+1} - v^n}{\triangle t} &= +\frac{u^{n+1} + u^n}{2}\Big[\mathrm{div}\Big(\frac{u\nabla v - v\nabla u}{u^2+v^2}\Big)\Big]^n, \end{aligned}$$

and similarly for (6) ($p = 1$).

Denoting by $(Div)^n$ an approximation of the expression $\mathrm{div}\Big(\frac{u\nabla v - v\nabla u}{u^2+v^2}\Big)$ evaluated at $(n\triangle t, ih, jh, ...)$, and solving the previous algebraic system in u^{n+1} and v^{n+1}, we obtain,

for both $p = 1$ and $p = 2$:

$$u^{n+1} = \frac{u^n - \left(2v^n + u^n \frac{\triangle t (Div)^n}{2}\right)\frac{\triangle t (Div)^n}{2}}{1 + \left(\frac{\triangle t (Div)^n}{2}\right)^2},$$

$$v^{n+1} = \frac{v^n + \left(2u^n - v^n \frac{\triangle t (Div)^n}{2}\right)\frac{\triangle t (Div)^n}{2}}{1 + \left(\frac{\triangle t (Div)^n}{2}\right)^2}.$$

To discretize the expression $\mathrm{div}\left(\frac{u\nabla v - v\nabla u}{u^2+v^2}\right)$, we use the finite difference scheme proposed in [24] for $\mathrm{div}\left(\frac{\nabla u}{|\nabla u|}\right)$, and which has also been used in [2] for a more general case.

Remark: As in the continuous case, it is easy to verify that the numerical solution exactly satisfies:

$$(u^{n+1})^2 + (v^{n+1})^2 = (u^n)^2 + (v^n)^2,$$

at any grid point x. This proves that the scheme produces bounded solutions independent of the relation between $\triangle t$ and h.

Remark: Note that we do not need to apply a renormalization step at every iteration. Only in the end of the algorithm we let $U = \frac{V}{|V|}$, with $V = (u, v)$. Note also that, if the initial data $V_0 = (u_0, v_0)$ already satisfies $|V_0| = 1$ everywhere, then, due to the previous remark, this equality will be preserved in time, and therefore, in the end, the numerical solution U will be directly given by V (in other words, in this case, there is no need to renormalize V at the steady state; we will simply have $U = V$).

Remark: Although the solutions remain bounded regardless of the magnitude of $\triangle t$, the numerical domain of dependence of u^{n+1}, v^{n+1} is such that convergence for $p = 2$ is only possible if $\triangle t \leq Ch^2$. This follows from the fact that θ satisfies the heat equation. We verified this by numerical experiments, and found that the quantity θ is noisy if $\triangle t$ is too large, although the solution is bounded (see Figure 7 for a comparison of results obtained for several values of $\triangle t$). Convergence for $p = 1$ requires a more restrictive constraint on $\triangle t$, typical of that for total variation minimization [24] in θ.

3 The S^2 case

We will follow the same idea as in the previous case, in order to derive the Euler-Lagrange equations associated with the unconstrained minimization problem (4), for any $M \geq 1$ and $N = 3$.

Using spherical coordinates, we let

$$U = (\cos\theta_1 \cos\theta_2, \cos\theta_1 \sin\theta_2, \sin\theta_1) \in S^2,$$

and

$$V = (r\cos\theta_1 \cos\theta_2, r\cos\theta_1 \sin\theta_2, r\sin\theta_1) = (u, v, w).$$

We then have $r^2 = u^2 + v^2 + w^2$,

$$\theta_1 = \tan^{-1}\left(\frac{w}{\sqrt{u^2+v^2}}\right),\ \theta_2 = \tan^{-1}\left(\frac{v}{u}\right),$$

and it can be shown that

$$|\nabla U|^2 = |\nabla\theta_1|^2 + \cos^2\theta_1 |\nabla\theta_2|^2.$$

Let us consider first the case $p = 2$. From

$$\inf_{\theta_1,\theta_2} \int_\Omega |\nabla\theta_1|^2 + \cos^2\theta_1 |\nabla\theta_2|^2 dx,$$

we obtain (parameterizing the descent directions by an artificial time t):

$$\theta_{1,t} = \triangle\theta_1 + \sin\theta_1 \cos\theta_1 |\nabla\theta_2|^2, \quad (7)$$

$$\theta_{2,t} = \mathrm{div}(\cos^2\theta_1 \nabla\theta_2). \quad (8)$$

Let us denote by E_1 and E_2 respectively, the expressions on the right-hand sides of (7) and (8), i.e.

$$\theta_{1,t} = E_1, \ \theta_{2,t} = E_2. \quad (9)$$

Again, from $r_t = 0$, we deduce that

$$uu_t + vv_t + ww_t = 0. \quad (10)$$

Computing and using

$$\nabla\theta_1 = \frac{(u^2+v^2)(\nabla w) - uw(\nabla u) - vw(\nabla v)}{(u^2+v^2+w^2)\sqrt{u^2+v^2}}, \quad (11)$$

$$\nabla\theta_2 = \frac{u(\nabla v) - v(\nabla u)}{u^2+v^2}, \quad (12)$$

we can then express E_1 and E_2 as functions of (u, v, w) by

$$E_1 = \triangle\theta_1 + \frac{w\sqrt{u^2+v^2}}{u^2+v^2+w^2}|\nabla\theta_2|^2, \quad E_2 = \mathrm{div}\Big(\frac{u(\nabla v) - v(\nabla u)}{u^2+v^2+w^2}\Big).$$

On the other hand, we have:

$$\theta_{1,t} = \frac{(u^2+v^2)w_t - uwu_t - vwv_t}{(u^2+v^2+w^2)\sqrt{u^2+v^2}}, \quad \theta_{2,t} = \frac{uv_t - vu_t}{u^2+v^2}.$$

We consider now the system formed by the equations (9), (10), in the unknowns u_t, v_t and w_t:

$$uu_t + vv_t + ww_t = 0, \quad \frac{(u^2+v^2)w_t - uwu_t - vwv_t}{(u^2+v^2+w^2)\sqrt{u^2+v^2}} = E_1, \quad \frac{uv_t - vu_t}{u^2+v^2} = E_2.$$

Solving this linear system in the unknowns u_t, v_t and w_t, we deduce the associated Euler-Lagrange equations:

$$u_t = -\frac{uw}{\sqrt{u^2+v^2}}E_1 - vE_2, \quad (13)$$

$$v_t = -\frac{vw}{\sqrt{u^2+v^2}}E_1 + uE_2, \quad (14)$$

$$w_t = \sqrt{u^2+v^2}E_1. \quad (15)$$

For the case $p = 1$ of the total variation minimization of Rudin-Osher-Fatemi [24], we consider first the problem in $\theta = (\theta_1, \theta_2) \in [-\frac{\pi}{2}, \frac{\pi}{2}]^2$:

$$\inf_{\theta_1,\theta_2} \int_\Omega \sqrt{|\nabla\theta_1|^2 + \cos^2\theta_1 |\nabla\theta_2|^2}\, dx,$$

which yields the equations:

$$\begin{aligned}
\theta_{1,t} &= \mathrm{div}\Big(\frac{\nabla\theta_1}{\sqrt{|\nabla\theta_1|^2 + \cos^2\theta_1|\nabla\theta_2|^2}}\Big) + \frac{\sin\theta_1\cos\theta_1|\nabla\theta_2|^2}{\sqrt{|\nabla\theta_1|^2 + \cos^2\theta_1|\nabla\theta_2|^2}}, \\
\theta_{2,t} &= \mathrm{div}\Big(\cos^2\theta_1 \frac{\nabla\theta_2}{\sqrt{|\nabla\theta_1|^2 + \cos^2\theta_1|\nabla\theta_2|^2}}\Big).
\end{aligned}$$

Denoting again by E_1 and E_2 the expressions on the right-hand sides of the above equations (corresponding now to the case $p = 1$), these can be expressed as functions of (u, v, w) using (11) and (12). The Euler-Lagrange equations for the case $p = 1$, in (u, v, w), are therefore as in (13)-(15), but with the corresponding differential operators E_1 and E_2 for $p = 1$.

3.1 The numerical algorithm for the S^2 case

The expressions E_1 and E_2 are discretized following [24] and [2], for both $p = 1$ and $p = 2$ (we will still denote their discretizations at a given point by E_1 and E_2).

Let us denote by u^n, v^n, w^n the discrete solutions at a discrete point, in two or three dimensions (but without writing $u^n_{i,j}$ or $u^n_{i,j,k}$, for simplicity). We discretize the system (13)-(15) using the following implicit scheme:

$$\begin{aligned}
u^{n+1} &= u^n - \frac{\triangle t}{\sqrt{(u^n)^2 + (v^n)^2}} u^n \Big(\frac{w^{n+1} + w^n}{2}\Big) E_1 - \Big(\frac{v^{n+1} + v^n}{2}\Big) E_2 \triangle t, \\
v^{n+1} &= v^n - \frac{\triangle t}{\sqrt{(u^n)^2 + (v^n)^2}} v^n \Big(\frac{w^{n+1} + w^n}{2}\Big) E_1 + \Big(\frac{u^{n+1} + u^n}{2}\Big) E_2 \triangle t, \\
w^{n+1} &= w^n + \triangle t \sqrt{(u^n)^2 + (v^n)^2}\, E_1.
\end{aligned}$$

We will use the notations: $A = \frac{E_1 \triangle t}{2\sqrt{(u^n)^2+(v^n)^2}}$, $B = \frac{E_2 \triangle t}{2}$, and $C = \triangle t \sqrt{(u^n)^2 + (v^n)^2} E_1$.

The linear system in $u^{n+1}, v^{n+1}, w^{n+1}$ is non-singular and has the unique solution:

$$u^{n+1} = \frac{R_1 - BR_2}{1 + B^2}, \quad v^{n+1} = \frac{R_2 + BR_1}{1 + B^2}, \quad w^{n+1} = w^n + C,$$

where $R_1 = u^n - Au^n(2w^n + C) - v^n B$ and $R_2 = v^n - Av^n(2w^n + C) + u^n B$.

Remark: The numerical scheme will exactly satisfy the relation: $(u^{n+1})^2 + (v^{n+1})^2 + (w^{n+1})^2 = (u^n)^2 + (v^n)^2 + (w^n)^2$ at each grid point, if in the above discretizations the expression $\sqrt{(u^n)^2 + (v^n)^2}$ is replaced by $\sqrt{u^n\Big(\frac{u^n+u^{n+1}}{2}\Big) + v^n\Big(\frac{v^n+v^{n+1}}{2}\Big)}$, but this yields a non-linear system in the unknowns u^{n+1}, v^{n+1} and w^{n+1}, which could be solved by a fixed-point iteration.

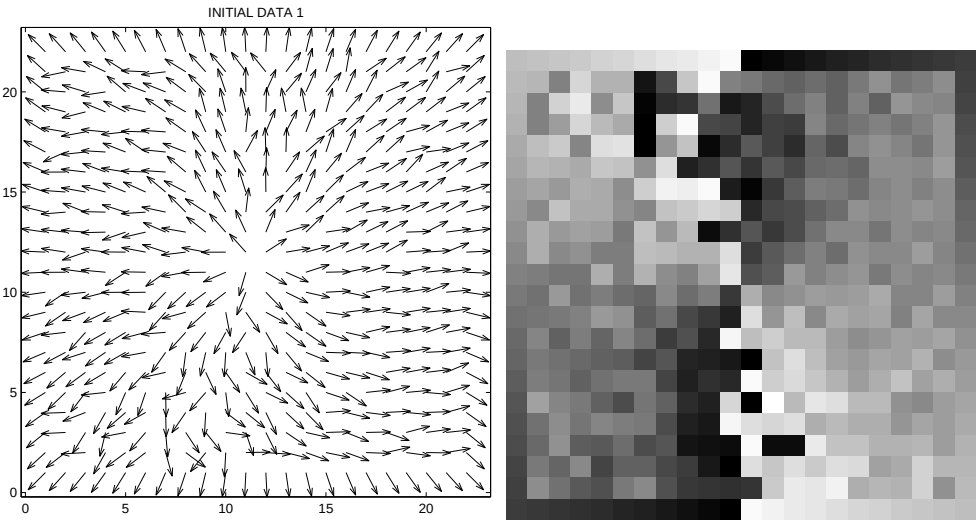

Figure 1: Left: initial condition for the Dirichlet problem, as a perturbation of $\frac{x-x_0}{|x-x_0|}$ in $(0,1)^2$, given by (16)-(17), and agreeing with $\frac{x-x_0}{|x-x_0|}$ at the boundary, where $x_0 = (0.5, 0.5)$. Right: corresponding initial angle $\theta = \tan^{-1}\left(\frac{v^0}{u^0}\right)$.

4 Numerical experiments

In this section we present numerical experiments in the cases $M = 2$, $N = 2$, and $M = 2, 3$ and $N = 3$. We will consider the cases with Dirichlet boundary conditions (subsection 4.1) and Neumann boundary conditions (subsection 4.2).

4.1 Numerical results for prescribed boundary conditions

In the S^1 case, we first consider the Dirichlet problem, with the boundary condition $U(x) = \frac{x-x_0}{|x-x_0|}$ on $\partial\Omega$, with $x_0 = (0.5, 0.5)$, where $\Omega = (0,1)^2$. In this case, it is known that the map $x \mapsto \frac{x-x_0}{|x-x_0|}$ is an exact solution and minimizer in $\overline{\Omega}$. We will show that the numerical solution has the correct behavior, approximating very well the exact solution.

Following [12], an initial condition $V^0 = (u^0, v^0)$ inside Ω can be a perturbation of $\frac{x-x_0}{|x-x_0|}$ (shown in Figure 1, after normalization):

$$u^0(x_1, x_2) = \frac{x_1 - .5}{|x - x_0|} + .6(1 + x_1^2 - x_2^2) - .8\eta, \tag{16}$$

$$v^0(x_1, x_2) = \frac{x_2 - .5}{|x - x_0|} + .6(x_1 - 2x_2) + .8\eta, \tag{17}$$

for all $(x_1, x_2) \in \Omega$, where η is random noise.

We will also consider another initial condition in this case, defined using the distance function to the boundary: for $(x, y) \in \Omega$, find $(x_b, y_b) \in \partial\Omega$ as the closest point to the boundary $\partial\Omega$ from (x, y). Then let $(u^0(x, y), v^0(x, y)) = U(x_b, y_b)$, where U defines the boundary conditions on $\partial\Omega$ (this second initial condition is shown in Figure 2).

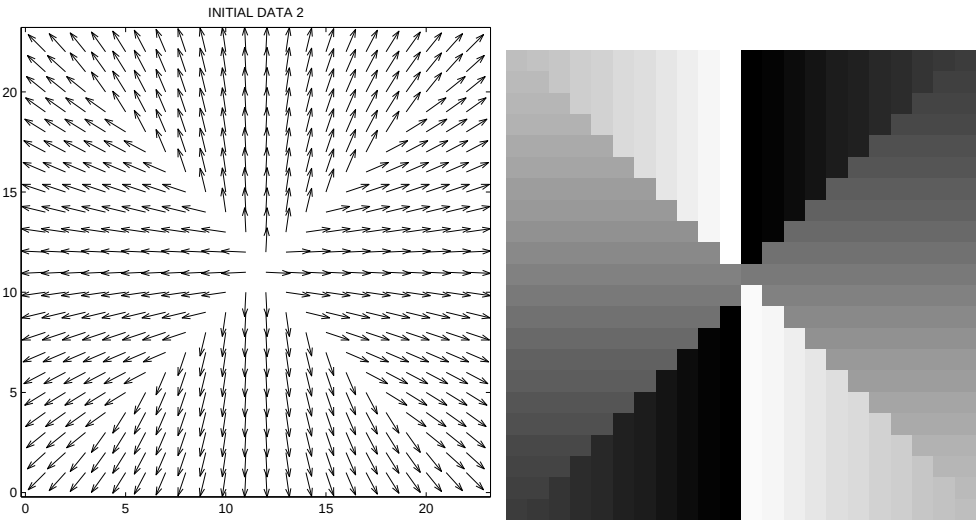

Figure 2: Left: another initial condition for the Dirichlet problem, constructed using the closest point to the boundary, and agreeing with $\frac{x-x_0}{|x-x_0|}$ at the boundary, where $x_0 = (0.5, 0.5)$. Right: corresponding initial angle $\theta = \tan^{-1}\left(\frac{v^0}{u^0}\right)$.

We consider now the case $p = 2$, for these two initial conditions. For the initial data 1, we also compare the results (the error and the energy decrease) with the classical harmonic map formulation with numerical renormalization at each time step, by solving the semi-discrete problem (using central difference approximations for the space derivatives, and with the same prescribed boundary conditions and the same time and space steps):

$$\begin{aligned}
\frac{u_*^{n+1} - u^n}{\triangle t} &= \triangle u^n + u^n\Big[(u_x^n)^2 + (u_y^n)^2 + (v_x^n)^2 + (v_y^n)^2\Big], \\
\frac{v_*^{n+1} - v^n}{\triangle t} &= \triangle v^n + v^n\Big[(u_x^n)^2 + (u_y^n)^2 + (v_x^n)^2 + (v_y^n)^2\Big], \\
(u^{n+1}, v^{n+1}) &= \frac{(u_*^{n+1}, v_*^{n+1})}{|(u_*^{n+1}, v_*^{n+1})|}.
\end{aligned}$$

We show the energy decrease and the error versus iterations for the results obtained with the classical harmonic maps applied to the initial data 1, and with the proposed model applied to both initial data 1 and 2 (see Figure 3). Using the proposed model, the error is much smaller. Also, note that the initial data 2 produces a result very fast. For both initial data 1 and 2, by our proposed model, the numerical solution $U(x) = \frac{V(x)}{|V(x)|}$ at steady state approximates very well the exact solution $\frac{x-x_0}{|x-x_0|}$ in $\Omega = [0, 1]^2$, and better than using the classical harmonic map scheme with the re-normalization at each step.

The results obtained with the proposed model for $p = 2$, for both data, are shown in Figure 4, together with the angle $\theta = \tan^{-1}\left(\frac{v}{u}\right)$.

Corresponding results obtained with the proposed model for $p = 1$ are shown in Figures 5 and 6.

In Figure 7 we show the angle $\theta = \tan^{-1}\left(\frac{v}{u}\right)$, obtained with the initial data 1, for $p = 2$, at steady state using the proposed model, for different decreasing values of $\triangle t$. This test proves

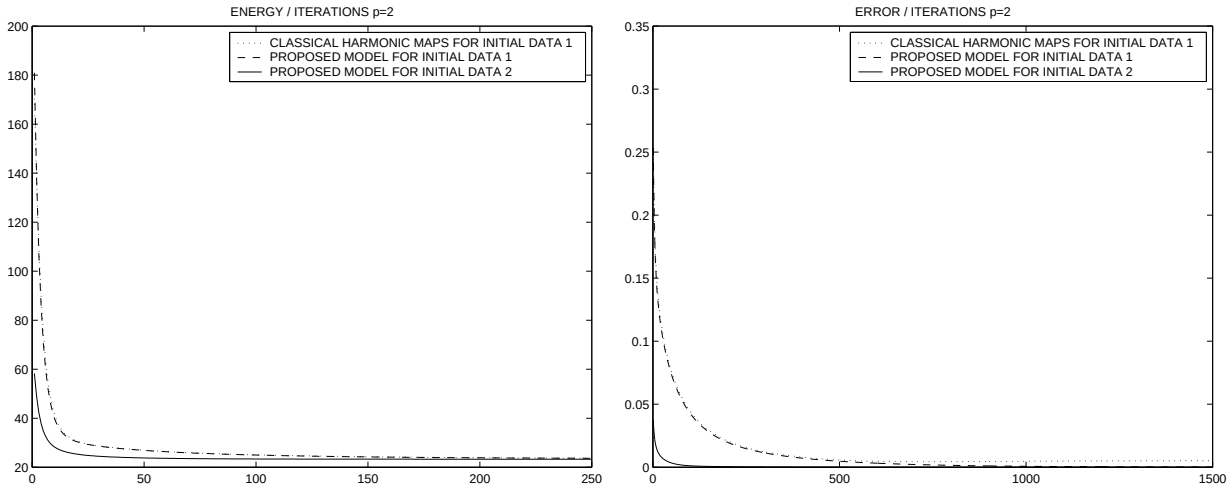

Figure 3: Energy and error versus iterations, for the classical harmonic map scheme applied to the initial data 1, and for the proposed model applied to both initial data 1 and 2. Note a much better accuracy obtained with the proposed model, compared with the classical formulation (we use the same $\triangle t = 0.0001$, $h = 1./21$), for both formulations.

again that, if $\triangle t$ is too large, then θ is noisy, but the numerical solution (u^n, v^n) remains bounded. Similar results can be obtained for $p = 1$, with a slightly stronger condition on $\triangle t$, to guarantee the stability of the numerical scheme.

We show next a numerical result for maps with values in S^2, in the three-dimensional case. Following [1], we perform a test, which shows again that, for the Dirichlet boundary conditions, the numerical solution approximates well the exact solution, for $p = 2$: in Figure 8, the initial data is to the left, and the result on the right. We see that the singularity has moved in the center of the domain, this being therefore an approximation of $\frac{x-x_0}{|x-x_0|}$, with $x_0 = (0.5, 0.5, 0.5)$.

4.2 Application to directional denoising and color image denoising

Next, we consider the case with Neumann boundary conditions. For the initial data in Figure 9, the results for $p = 1$ and $p = 2$ are presented in Figure 10. Note that, for $p = 1$ (left), the "edges" are very well preserved, thanks to the total variation minimization [24], while denoising in the homogeneous regions (we show the results at steady state, and without any fitting term).

Finally, we show applications more related to denoising of color RGB images. In the first test (Figure 11), we consider a map from $\mathbb{R}^2 \to S^2$, but instead of vectors, we plot colors, using the rectangular color space RGB: in Figure 11 left, we show an initial image of noisy directions (the components of the unit vector (u, v, w) are visualized as channels in a color RGB picture). We show in Figure 11 middle and right, two numerical results in the case of directional diffusion, with $p = 1$ (middle) and $p = 2$ (right), with Neumann boundary conditions. As expected, in the case of the total variation [24], the edges are well preserved, while these are smeared out with the heat flow.

We end the paper with an application to denoising of color RGB images. We consider

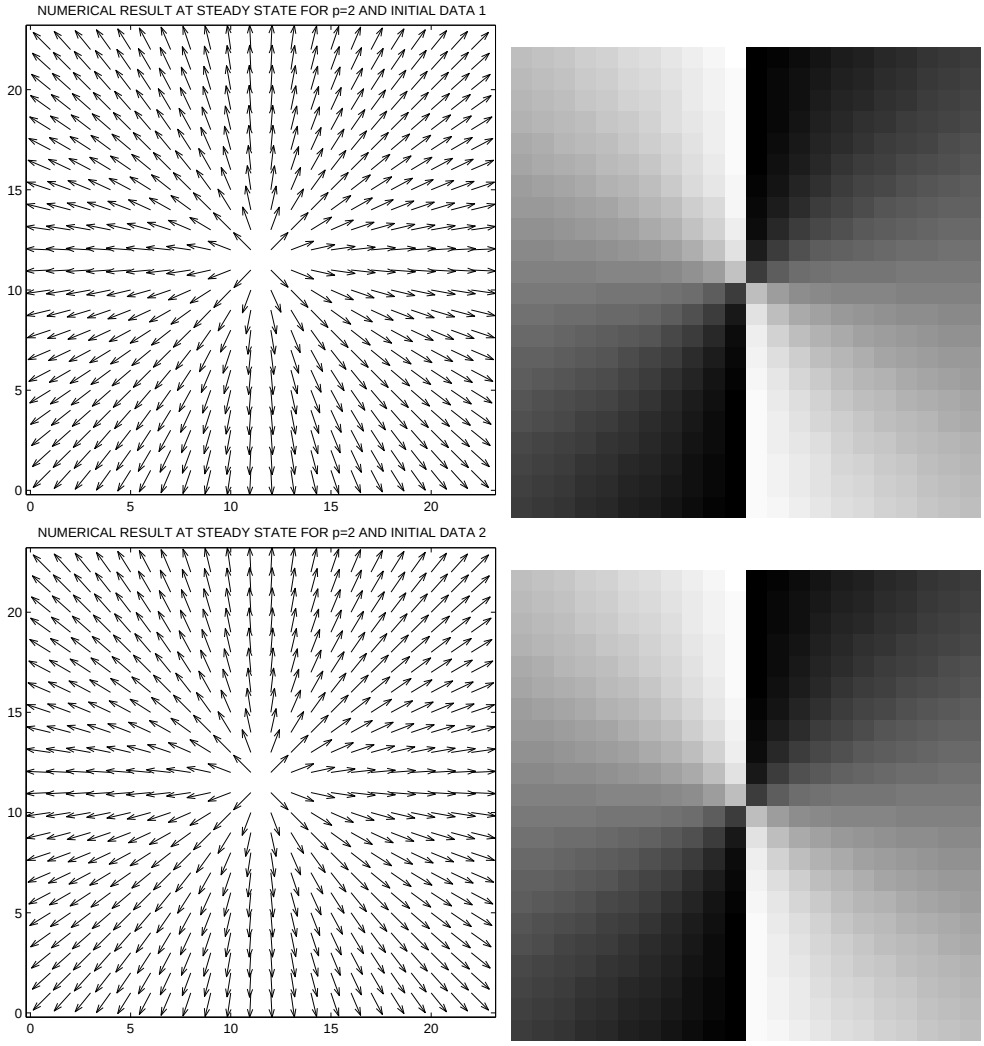

Figure 4: Left: numerical result, approximating well the exact solution and minimizer for $p = 2$, with Dirichlet boundary conditions ($\triangle t = 0.0001$, $h = 1/21$). Right: corresponding angle $\theta = \tan^{-1}\left(\frac{v}{u}\right)$.

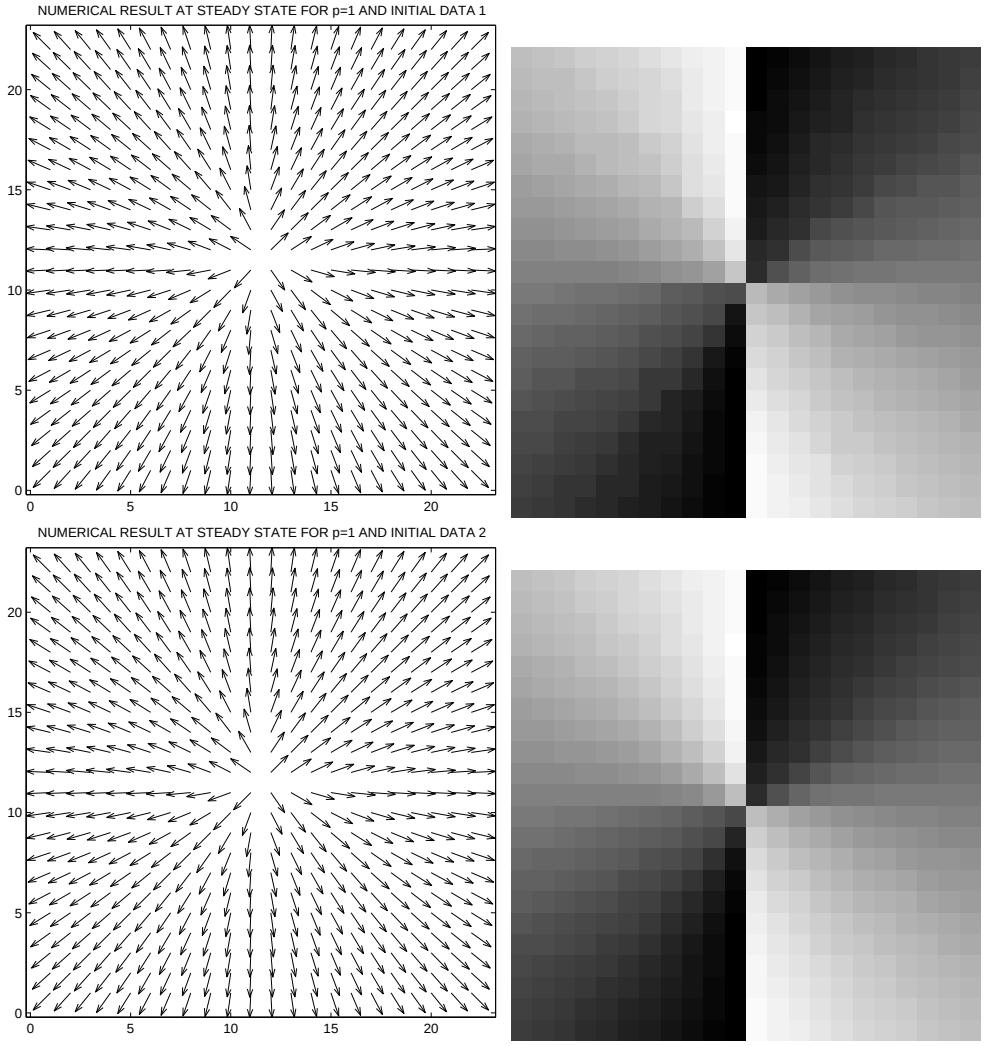

Figure 5: Left: numerical result, approximating well the exact solution and minimizer for $p = 1$, with Dirichlet boundary conditions ($\triangle t = 0.00001$, $h = 1/21$). Right: corresponding angle $\theta = \tan^{-1}\left(\frac{v}{u}\right)$.

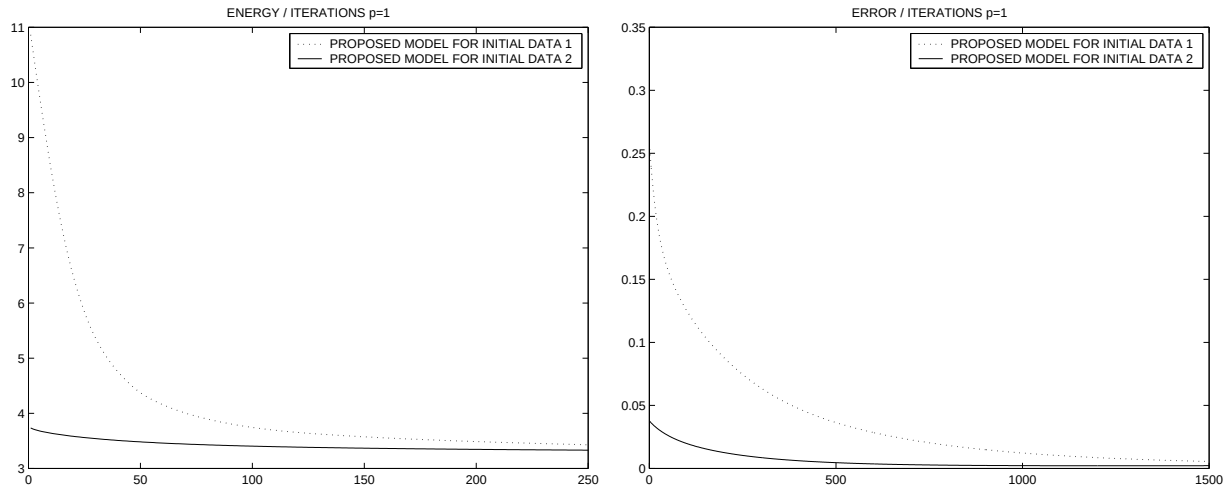

Figure 6: Energy and error versus iterations for $p = 1$ with Dirichlet boundary conditions, corresponding to the results in Figure 5.

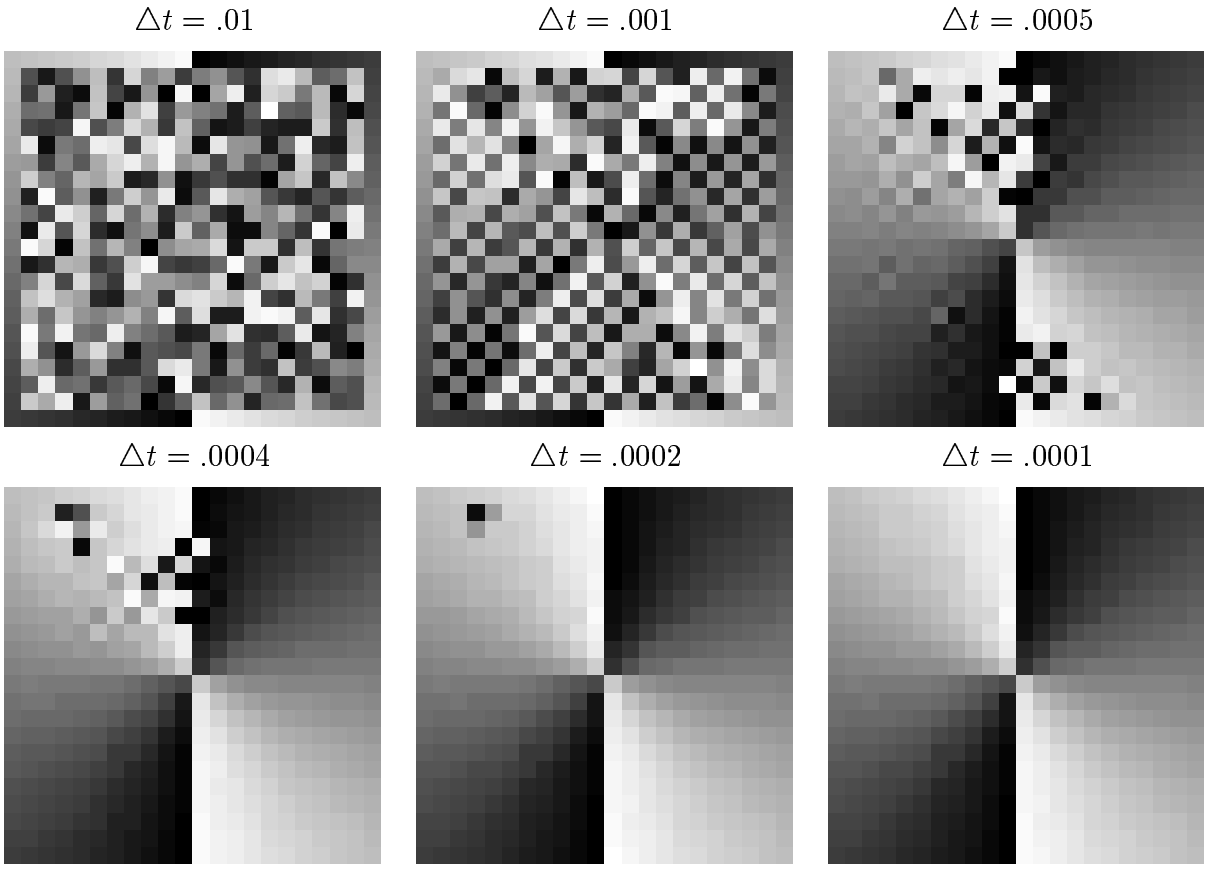

Figure 7: The angle $\theta = tan^{-1}\left(\frac{v}{u}\right)$ at steady state for $p = 2$, obtained using the proposed model with Dirichlet boundary conditions, for decreasing values of $\triangle t$ (if $\triangle t$ is too large, θ is noisy, but the numerical solution (u^n, v^n) always remains bounded).

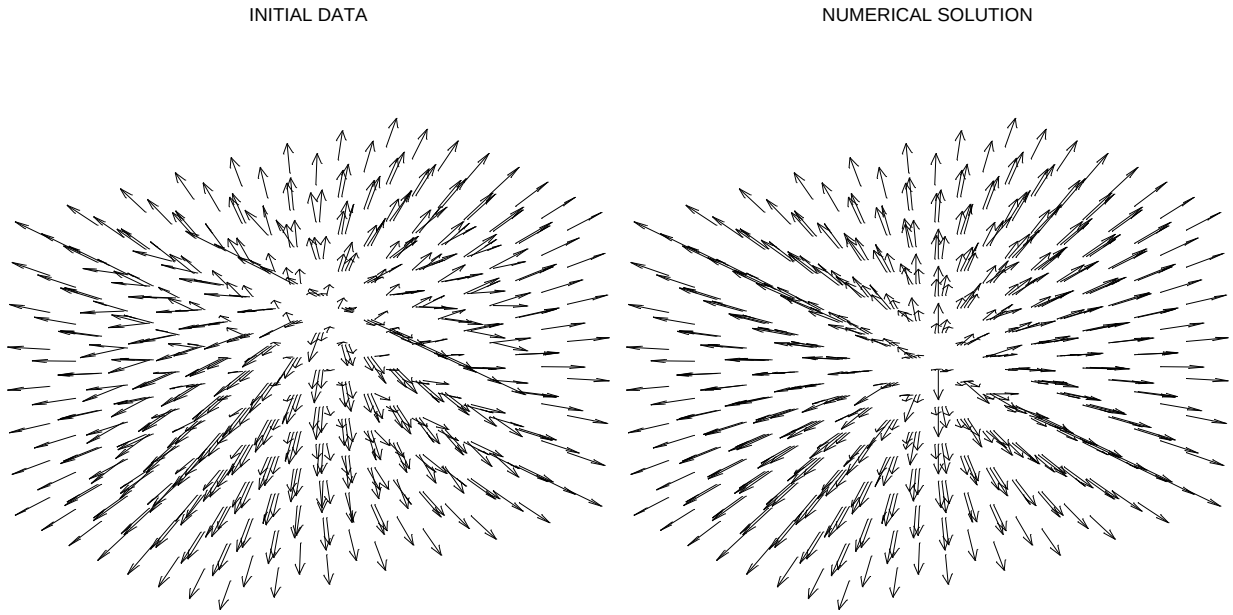

Figure 8: Left: initial flow $\frac{x-x_1}{|x-x_1|}$ from $(0,1)^3$ into S^2 with prescribed Dirichlet boundary conditions equal to $\frac{x-x_0}{|x-x_0|}$, where $x_0 = (0.5, 0.5, 0.5)$ and $x_1 = (0.64, 0.64, 0.64)$. Right: numerical solution obtained for $p = 2$. The singularity has moved to the center of the domain, approximating well the exact solution and minimizer ($\triangle t = 0.00001$, $h = 1/7$).

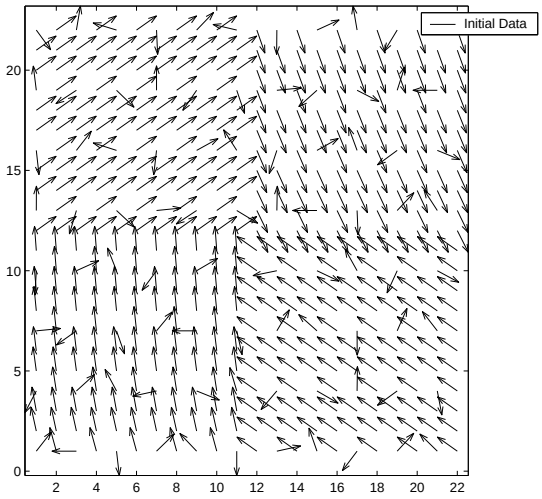

Figure 9: Initial noisy data for the case with Neumann boundary conditions.

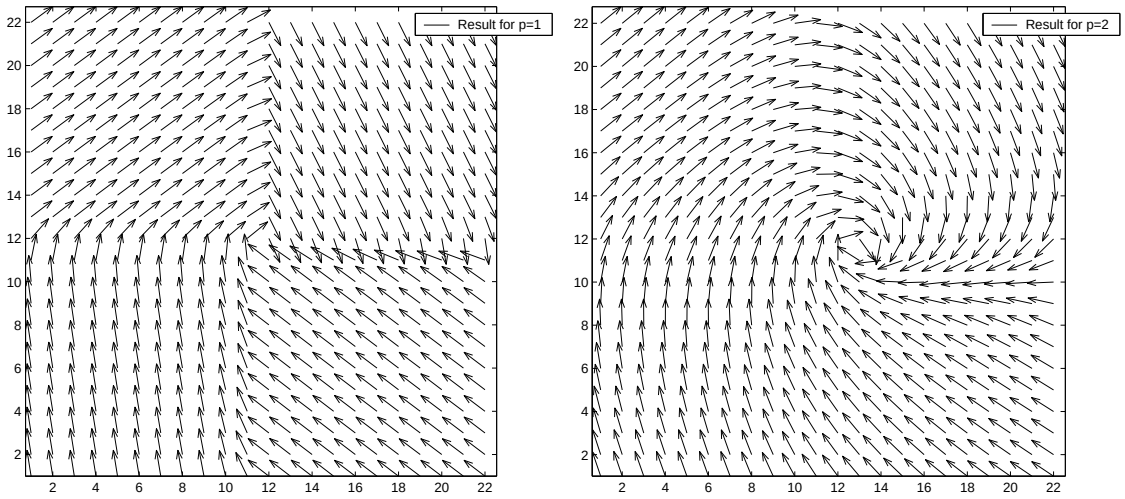

Figure 10: Numerical results with the initial noisy data from Figure 9, for Neumann boundary conditions and $p = 1$ (left), with $\triangle t = 0.00005$, $h = 1$, steady state, and $p = 2$ (right), with $\triangle t = 0.00005$, $h = 1$, steady state.

a color image $I = (I_R, I_G, I_B) \in I\!R^3$, from which we can extract the intensity or brightness $|I| = \sqrt{I_R^2 + I_G^2 + I_B^2}$ and the chromaticity $\frac{I}{|I|} = \left(\frac{I_R}{\sqrt{I_R^2+I_G^2+I_B^2}}, \frac{I_G}{\sqrt{I_R^2+I_G^2+I_B^2}}, \frac{I_B}{\sqrt{I_R^2+I_G^2+I_B^2}}\right) \in S^2$. Let us assume that noise has been added to the image, but only to the chromaticity $\frac{I}{|I|}$. Then, we can apply the above directional denoising method, with $p = 1$, to the chromaticity (in this test case, we do not add noise to the brightness $|I|$). If noise were also added to the brightness, then this could have been denoised, for example, with the corresponding Total Variation minimization [24], or any other anisotropic diffusion PDE. With the processed result, we obtain a denoised version of the image, using the unchanged brightness. We mention that the idea of decomposing a color RGB image into its brightness and chromaticity, and processing these two quantities separately, has been already used in other works, for example in [19], [37], [38], [35], [36], [9], [25], [26], [30].

This type of application is illustrated in the last numerical example. In Figure 12, we show an original color RGB image $I = (I_R, I_G, I_B) \in I\!R^3$ (left), a noisy version (middle), where only the directions $\frac{I}{|I|}$ (the chromaticity) were noisy, keeping the brightness $|I|$ or magnitude of the vectors unchanged, and a denoised version obtained with $p = 1$ (right), where only the chromaticity or directions were denoised, keeping the brightness or magnitude unchanged from the original image, equal to $|I|$.

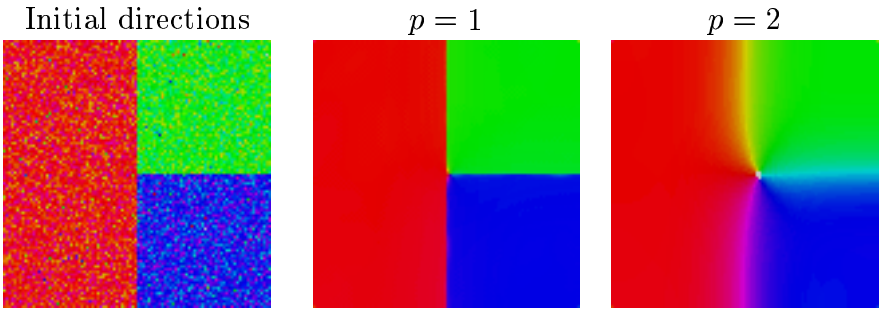

Figure 11: Directions denoising with $p = 1$ (middle) and $p = 2$ (right). The unit vectors are represented as RGB colors ($\triangle t = 0.01$, $h = 1$).

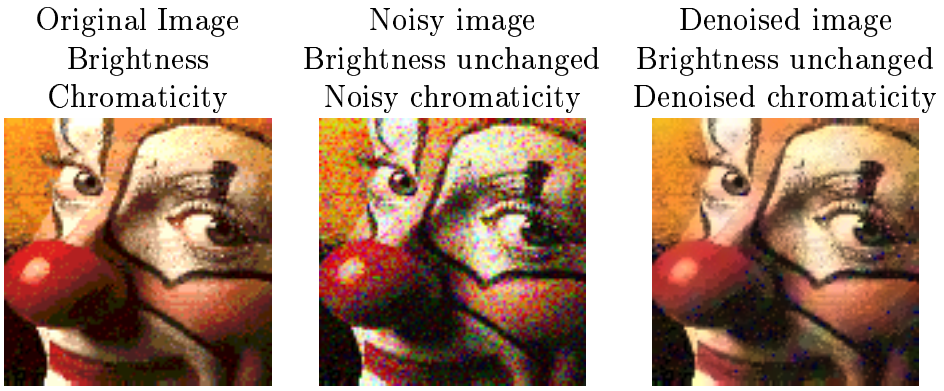

Figure 12: Chromaticity denoising with $p = 1$. The brightness is kept unchanged from the original image ($\triangle t = 0.01$, $h = 1$, 50 iterations).

5 Concluding remarks and discussions for more general manifolds

In this paper, we have proposed an alternative approach for computing harmonic maps and harmonic flows. We have illustrated the proposed methods by experimental results and comparisons with classical schemes, and applications to directional diffusion and image processing.

It is easy to see that that the minimization problems (1) and (4) have the same infimum, and that solving one problem, yields a minimizer for the other one, and vice-versa. Of course we cannot expect to have uniqueness of minimizers for (4), because λV is a minimizer for any non-zero constant λ, if V is a minimizer. Showing the existence of minimizers for (4) may be a difficult problem, because the energy is not convex. We have also posed the question: given Dirichlet boundary conditions on $\partial\Omega$, what would be a good initial condition in Ω to guarantee a fast computation of a minimizer (to find a particular initial condition, we have used the distance function to the boundary $\partial\Omega$, although perhaps other choices could also be constructed).

This method can be extended to more general manifolds. For instance, if we consider a manifold $\mathcal{M} \subset I\!R^N$, then the associated constrained minimization problem can be formulated as follows:

$$\inf_{U:\Omega\to\mathcal{M}} F(U) = \int_\Omega |\nabla U|^p dx.$$

The proposed method for the case when $\mathcal{M} = S^{N-1}$ can be extended to such general cases, if we assume for example that $\mathcal{M}$ can be represented implicitly, via a level set function, given by the signed distance function to $\mathcal{M}$, from any other point in $I\!R^N$ (we refer to [22] for definitions and dynamics of closed hyper-surfaces defined implicitly, via level set functions and signed distance functions). Then we can write $\mathcal{M} = \{x \in I\!R^N : \ d(x) = 0\}$, where d is the signed distance function to $\mathcal{M}$ (in particular a Lipschitz function, taking real values). To any $U : \Omega \to \mathcal{M}$, we associate $V : \Omega \to I\!R^N$, such that U is the projection of V on the manifold $\mathcal{M}$. This can be done using the closest point or the projection $U = V - d(V)\nabla_V d(V)$, and we have $d(U) = 0$. Then, we can associate the unconstrained minimization problem:

$$\inf_{V:\Omega\to I\!R^N} \int_\Omega |\nabla(V - d(V)\nabla_V d(V))|^p dx.$$

This is a generalization of the case $\mathcal{M} = S^{N-1}$, because in this case, we have $d(V) = |V| - 1$, and $V - d(V)\nabla_V d(V) = \frac{V}{|V|}$. We plan to consider in the future the solution of this general unconstrained minimization problem.

We would like to mention that the case of more general manifolds, and in particular of manifolds defined implicitly, has been considered in [3], [4], for the manifold of origin, and in [21] for the target manifold, but using different formulations.

We would also like to mention that the idea of solving constrained minimization problems for harmonic maps by associating unconstrained minimization problems, has been used as a theoretical tool by Y. Chen, F.-H. Lin and M. Struwe [10], [11], [34]. They find a smooth energy-minimizing harmonic map U as weak limit of minimizers U_L to an unconstrained variational problem, for $L \to \infty$. They construct in a different way the unconstrained variational problems.

Acknowledgments

The authors would like to thank Guillermo Sapiro, for his interest in this work and for his very useful remarks and suggestions. The authors started to work on this subject after one of his visits at UCLA. We also thank him for providing us the "clown" picture. We would also like to thank Ron Kimmel, for interesting discussions and for pointing out to us some related references. Finally, we are grateful to the first unknown referee for his numerous typographical and stylistic corrections, helping to improve the presentation of the paper.

Appendix

We show here that, parameterizing the descent direction by an artificial time, the energy is still decreasing under the associated flow (see the last remark from subsection 2.1). We show this property in a general framework. In order to solve the minimization problem

$$\inf_{u_1,...,u_N} \int_\Omega f(u_1,...,u_N,\nabla u_1,...,\nabla u_N)dx,$$

where $\Omega \subset I\!R^N$, $x=(x_1,...,x_M) \in I\!R^M$, we associate the time-dependent coupled PDE's, for $1 \leq i \leq N$ (the functions u_i take real values, and we use the notations $u=(u_1,...,u_N)$, $\nabla u = (\nabla u_1,...,\nabla u_N)$, $(u_i)_{x_j} = \frac{\partial u_i}{\partial x_j}$):

$$\frac{\partial u_i}{\partial t} = -\frac{\partial f(u,\nabla u)}{\partial u_i} + \sum_{j=1}^{M} \frac{\partial}{\partial x_j}\Big(\frac{\partial f(u,\nabla u)}{\partial((u_i)_{x_j})}\Big),$$

with the initial conditions $u_i(0,x) = u_{0,i}(x)$ in Ω. On the boundary $\partial\Omega$, we can assume Dirichlet boundary conditions $u_i(t,x) = u_{0,i}(x)$ for $x \in \partial\Omega$ and $t > 0$, or free boundary conditions in the form $\sum_{j=1}^{M} \frac{\partial f(u,\nabla u)}{\partial((u_i)_{x_j})} n_j = 0$, where $\vec{n} = (n_1,...,n_M)$ is the exterior unit normal to $\partial\Omega$.

We formally compute now $\frac{d}{dt}\int_\Omega f(u_1,...,u_N,\nabla u_1,...,\nabla u_N)dx = \frac{d}{dt}\int_\Omega f(u,\nabla u)dx$ and we show that this quantity is always negative or zero, therefore the energy is decreasing in time:

$$\begin{aligned}
\frac{d}{dt}\int_\Omega f(u,\nabla u)dx &= \sum_{i=1}^{N}\int_\Omega \Big(\frac{\partial f(u,\nabla u)}{\partial u_i}\Big)\Big(\frac{\partial u_i}{\partial t}\Big)dx + \sum_{i=1}^{N}\int_\Omega \Big[\sum_{j=1}^{M}\Big(\frac{\partial f(u,\nabla u)}{\partial((u_i)_{x_j})}\Big)\Big(\frac{\partial (u_i)_{x_j}}{\partial t}\Big)\Big]dx \\
&= \sum_{i=1}^{N}\int_\Omega \Big(\frac{\partial f(u,\nabla u)}{\partial u_i}\Big)\Big(\frac{\partial u_i}{\partial t}\Big)dx + \sum_{i=1}^{N}\int_\Omega \Big[\sum_{j=1}^{M}\Big(\frac{\partial f(u,\nabla u)}{\partial((u_i)_{x_j})}\Big)\Big(\frac{\partial (u_i)_t}{\partial x_j}\Big)\Big]dx \\
&= \sum_{i=1}^{N}\int_\Omega \Big(\frac{\partial f(u,\nabla u)}{\partial u_i}\Big)\Big(\frac{\partial u_i}{\partial t}\Big)dx + \sum_{i=1}^{N}\int_\Omega \Big\{-\sum_{j=1}^{M}\Big[\frac{\partial}{\partial x_j}\Big(\frac{\partial f(u,\nabla u)}{\partial((u_i)_{x_j})}\Big)\Big]\Big(\frac{\partial u_i}{\partial t}\Big)\Big\}dx \\
&\qquad + \sum_{i=1}^{N}\Big\{\int_{\partial\Omega}\Big(\frac{\partial u_i}{\partial t}\Big)\Big(\sum_{j=1}^{M}\frac{\partial f(u,\nabla u)}{\partial((u_i)_{x_j})}n_j\Big)dS\Big\} \\
&= \sum_{i=1}^{N}\int_\Omega \Big(\frac{\partial u_i}{\partial t}\Big)\Big[\frac{\partial f(u,\nabla u)}{\partial u_i} - \sum_{j=1}^{M}\frac{\partial}{\partial x_j}\Big(\frac{\partial f(u,\nabla u)}{\partial((u_i)_{x_j})}\Big)\Big]dx = -\sum_{i=1}^{N}\int_\Omega \Big(\frac{\partial u_i}{\partial t}\Big)^2 dx \;\leq\; 0.
\end{aligned}$$

References

[1] F. Alouges, *A new algorithm for computing liquid crystal stable configurations: the harmonic mapping case*, SIAM J. Num. Anal. Vol. 34(5): 1708-1726, 1997.

[2] G. Aubert and L. Vese, *A variational method in image recovery*, SIAM J. Num. Anal., Vol. 34(5): 1948-1979, 1997.

[3] M. Bertalmio, G. Sapiro, L.-T. Cheng and S. Osher, *Variational problems and partial differential equations on implicit surfaces*, Proceedings 1st IEEE Workshop on Variational and Level Set Methods in Computer Vision, 186 -193, 2001.

[4] M. Bertalmio, L.-T. Cheng, S. Osher and G. Sapiro, *Variational problems and partial differential equations on implicit surfaces*, Journal of Computational Physics, 174 (2):759-780, 2001.

[5] F. Bethuel, H. Brezis and J.M. Coron, *Relaxed energies for harmonic maps*, in: H. Beresticky, J.M. Coron, I. Ekeland (Eds.), Variational Problems, Paris, Birkhauser, Basel, June 1988.

[6] F. Bethuel, H. Brezis and F. Helein, *Asymptotics for the minimization of a Ginzburg-Landau functional*, Calculus of Variations and Partial Differential Equations 1(2), pp. 123-148, 1993.

[7] F. Bethuel, H. Brezis and F. Helein, *Singular limit for the minimization of Ginzburg-Landau functionals*, CRAS I-MATH 314 (12), pp. 891-895, 1992.

[8] H. Brezis, J.M. Coron and E.H. Lieb, *Harmonic maps with defects*, Communications in Mathematical Physics 107, pp. 649-705, 1986.

[9] T. Chan and J. Shen, *Variational restoration of nonflat image features: models and algorithms*, SIAM J. Appl. Math., 61(4): 1338-1361, 2000.

[10] Y. Chen and F.-H. Lin, *Remarks on approximate harmonic maps*, Comm. Math. Helv. 70, pp. 161-169, 1995.

[11] Y. Chen and M. Struwe, *Existence and partial regularity results for the heat flow for harmonic maps*, Math. Z. 201, pp. 83-103, 1989.

[12] R. Cohen, R. Hardt, D. Kinderlehrer, S.-Y. Lin, and M. Luskin, *Minimum energy configurations for liquid crystals: computational results*, in Theory and Applications of Liquid Crystals, IMA 5, Springer-Verlag, 99-122, 1997.

[13] J.M. Coron and R. Gulliver, *Minimizing p-harmonic maps into spheres*, J. reine angew. Math. 401, 82-100, 1989.

[14] P. Courilleau and F. Demengel, *Heat flow for p-harmonic maps with values in the circle*, Nonlinear Analysis - Theory Methods & Applications, 41 (5-6): 689-700, 2000.

[15] P. Courilleau, S. Dumont, and R. Hadiji, *Regularity of minimizing maps with values in S^2 and some numerical simulations*, CMLA-ENS Technical Report 9905, 1999.

[16] B. Dacorogna, I. Fonseca, J. Maly, K. Trivisa, *Manifold constrained variational problems*, Calc. Var. 9: 185-206, 1999.

[17] W. E and X.-P. Wang, *Numerical methods for the Landau-Lifshitz equation*, SIAM J. Numer. Anal., 38(5): 1647-1665, 2000.

[18] M. Giaquinta, G. Modica and J. Soucek, *Variational problems for maps of bounded variation with values in S^1*, Cal. Var. 1, pp. 87-121, 1993.

[19] D. Karakos and P.E. Trahanias, *Generalized multi-channel image-filtering structures*, IEEE Transactions Image Processing 6(7): 1038-1045, 1997.

[20] R. Kimmel, R. Malladi, N. Sochen, *Images as Embedded Maps and Minimal Surfaces: Movies, Color, Texture, and Volumetric Medical Images*, IJCV 39(2): 111-129, 2000.

[21] F. Memoli, G. Sapiro, and S. Osher, *Solving Variational Problems and Partial Differential Equations Mapping into General Target Manifolds*, UCLA CAM Report 02-04, 2002.

[22] S. Osher and J. Sethian, *Fronts Propagating with Curvature-Dependent Speed: Algorithms Based on Hamilton-Jacobi Formulation*, Journal of Computational Physics, 79: 12-49, 1988.

[23] P. Perona, *Orientation diffusion*, IEEE Trans. on Image Processing 7: 457-467, 1998.

[24] L. Rudin, S. Osher, E. Fatemi, *Nonlinear total variation based noise removal algorithms*, Physica D 60: 259-268, 1992.

[25] N.A. Sochen and R. Kimmel, *Combing a Porcupine via Stereographic Direction Diffusion*, in M. Kerckhove (Ed.): Scale-Space 2001, LNCS 2106: 308-316, 2001.

[26] R. Kimmel and N. Sochen, *Orientation diffusion or how to comb a porcupine*, Journal of Visual Communication and Image Representation, 13 (1-2): 238-248, 2002.

[27] R. Schoen and K. Uhlenbeck, *A regularity theory for harmonic maps*, J. Diff. Geom. 17, pp. 307-335, 1982.

[28] R. Schoen and K. Uhlenbeck, *Boundary regularity and the Dirichlet problem for harmonic maps*, J. Diff. Geom. 18, pp. 253-268, 1983.

[29] R. Schoen and K. Uhlenbeck, *Regularity of minimizing harmonic maps into the sphere*, Invent. Math. 78, pp. 89-100, 1984.

[30] N. Sochen, R. Kimmel and R. Malladi, *A General Framework for Low Level Vision*, IEEE Transactions on Image Processing, 7(3): 310-318, 1998.

[31] M. Struwe, *On the evolution of harmonic mappings of Riemannian surfaces*, Comment. Math. Helvetici 60, 558-581, 1985.

[32] M. Struwe, *Variational Methods*, Springer Verlag, New York, 1990.

[33] M. Struwe, *The evolution of harmonic maps, existence, partial regularity and singularities*, Nonlinear Differential Equations and Applications 7,00 pp: 485-491, 1992.

[34] M. Struwe, *Uniqueness of harmonic maps with small energy*, Manuscripta Math. 96, pp. 463-486, 1998.

[35] B. Tang, G. Sapiro, and V. Caselles, *Diffusion of General Data on Non-Flat Manifolds via Harmonic Maps Theory: The Direction Diffusion Case*, Int. J. of Computer Vision 36(2): 149-161, 2000.

[36] B. Tang, G. Sapiro, and V. Caselles, *Color Image Enhancement via Chromaticity Diffusion*, IEEE Transactions on Image Processing, 10(5): 701-707, 2001.

[37] P.E. Trahanias and A.N. Venetsanopoulos, *Vector directional filters - A new class of multichannel image processing filters*, IEEE Transactions Image Processing 2(4): 528-534, 1993.

[38] P.E. Trahanias, D. Karakos, and A.N. Venetsanopoulos, *Directional processing of color images: Theory and experimental results*, IEEE Transactions Image Processing 5(6): 868-880, 1996.

[39] D. Tschumperle and R. Deriche, *Regularization of Orthonormal Vector Sets Using Coupled PDE's*, Proceedings 1st IEEE Workshop on Variational and Level Set Methods in Computer Vision, 3-10, 2001.